Thermochimica Acta 574 (2013) 1–9

Contents lists available at ScienceDirect

Thermochimica Acta

journal homepage: www.elsevier.com/locate/tca

Inverse analysis of wood pyrolysis with long residence times in the temperature range 210–290 °C: Selection of multi-step kinetic models based on mass loss residues

Sofien Cavagnol[a,b], Elena Sanz[a,*], Willi Nastoll[a], John F. Roesler[a], Victor Zymla[b], Patrick Perré[b]

[a] *IFP Energies nouvelles – Lyon, Rond point de L'échangeur de Solaize – BP 3, 69360 Solaize, France*
[b] *École Centrale Paris, LGPM, Grande Voie des Vignes, 92295 Chatenay-Malabry, France*

ARTICLE INFO

Article history:
Received 3 June 2013
Received in revised form 9 September 2013
Accepted 10 September 2013
Available online 10 October 2013

Keywords:
Pyrolysis
Torrefaction
Biomass
Kinetic simulation
Inverse method

ABSTRACT

The aim of this paper is to evaluate different types of kinetic models and to propose a set of kinetic parameters for simulating the heat treatment of woody biomass under temperatures representative of torrefaction conditions. The mass loss of three wood types, locust, spruce and eucalyptus, as well as their main components, cellulose, xylan, glucomannan and lignin, has been determined in a TGA at different isothermal temperatures between 210 and 290 °C for residence times of up to ten hours. These data were used to evaluate the kinetic parameters corresponding to various multi-step series reaction mechanisms proposed in the literature. A computational solution of the multi-step formulation was derived, which allows the exact conditions undergone by the sample to be used as input parameters. The inverse procedure takes into account simultaneously the different temperature levels for each species. A comprehensive table summarizes all results, among which the dimensionless residues, proposed as a guideline to choose the relevant mechanism complexity. Overall we find that 2-step series reaction models provide acceptable accuracy for reproducing the mass loss from lignocellulosic biomass and their constituents under torrefaction conditions.

© 2013 Elsevier B.V. All rights reserved.

1. Introduction

Lignocellulosic biomass is considered as a potential renewable carbon neutral source of liquid fossil fuels. Various transformation processes exist, among which the BtL (biomass to liquid) process in which the first step requires the biomass to be pulverized into an EFR (entrained flow reactor) for gasification. The main difficulty is that lignocellulosic biomass is a fibrous and resilient material which is costly to grind and complicated to inject, two negative aspects regarding the efficiency of the BtL chain.

Torrefaction is a mild thermal treatment at temperatures ranging from 200 to 300 °C under an inert atmosphere and with residence times of about 30–60 min. The process produces a material that has several advantages: it is easily ground to powders with good fluidization properties [1], it is hydrophobic and thus less sensitive to humidity upon storage [2,3] and it has increased LHV/HHV values [4,5]. The main drawback is the overall energy loss of the process. A compromise must therefore be found between improved physical properties of the treated material and acceptable energy loss. The extent of mass loss during torrefaction can be used as a first indicator of the alterations of biomass properties [5]. Since this loss is a strong function of the temperature history of the biomass, accurate kinetic models are a requirement for optimizing industrial operating conditions.

Many kinetic models for biomass thermal treatment and for its main components (cellulose, hemicellulose and lignin) have been proposed in the literature with various degrees of complexity and are briefly reviewed hereafter.

1.1. *Models proposed for wood*

Early models [6] assumed the thermal treatment of wood to proceed via a single first order reaction giving a solid product and a gas phase. The mass loss rate is given by Eq. (1) where $k(T)$ is the kinetic constant and follows the Arrhenius law as given in Eq. (2). The extent of conversion, α, is defined in Eq. (3) where X_{io} is the initial mass of woody biomass, X_i is the mass of the wood as a function of time and X_{inf} is the mass of wood at the end of the experiment (thermally treated wood). In the case of isothermal tests, the hypothesis of a first order reaction ($n = 1$) allows Eq. (1) to be solved analytically to determine the rate parameters A, E and n, while in

---

* Corresponding author. Tel.: +33 437702337; fax: +33 437702008.
E-mail address: elena.sanz@ifpen.fr (E. Sanz).

0040-6031/$ – see front matter © 2013 Elsevier B.V. All rights reserved.
http://dx.doi.org/10.1016/j.tca.2013.09.009

Table 1
Kinetic constant parameters identified using Eq. (4) for pine and beech [7].

Type of wood	Heating rate (K/min)	Temperature (°C)	E (kJ/mol)	A (s^{-1})
Beech	10	261–382	118	3.32×10^9
	15	260–402	117	2.98×10^9
	20	270–394	120	6.68×10^9
	30	280–406	122	1.14×10^{10}
	40	284–408	124	1.9×10^{10}
Pine	10	270–408	120	3.56×10^9
	15	272–425	114	1.26×10^9
	20	270–450	101	9.02×10^7
	30	278–458	103	1.51×10^8
	40	278–456	103	2.32×10^8

the case of a dynamic tests with temperature ramps, the plot of the left hand term of Eq. (4) as a function of $1/T$ can be used.

$$\frac{d\alpha}{dt} = k(T)f(\alpha) = k(T)(1-\alpha)^n \tag{1}$$

$$k(T) = A\exp\left(\frac{-E}{RT}\right) \tag{2}$$

$$\alpha = \frac{X_{i0} - X_i}{X_{i0} - X_{inf}} \tag{3}$$

$$\ln\left(\frac{d\alpha/dt}{1-\alpha}\right) = \frac{\ln A - E}{RT(t)} \tag{4}$$

Table 1 summarizes rate constant parameters identified by this method for thermal treatment of beech and pine [7] up to 400 °C with a constant heating rate varying from 10 to 40 K/min. The values of E and A for beech are observed to increase with the heating rate, whereas the contrary is observed for pine. The variation of kinetic parameters with the heating rate when using a single step first order reaction has also been observed in coal pyrolysis [8] and is explained by the fact that coal devolatilization at the molecular level proceeds through a complex set of parallel and series reactions. Lignocellulosic biomass is expected to behave somewhat like coal in the sense that it also should evolve through many different reactions due to its complex molecular structure [9]. Clearly a single-step reaction cannot be appropriate for describing the kinetics under all conditions.

More recently Branca and di Blasi [10] proposed a three step kinetic model for wood thermal treatment in the temperature range of 265–435 °C as shown in Table 2 (scheme C). In this scheme, X is the wood, S is the thermally treated wood, V_1, V_2 and V_3 are volatiles, X′ and X″ are intermediate components. The transformation was assumed to occur through three successive single first order reactions. Kinetic parameters were identified with several isothermal tests lasting 90 min after heating at 1000 K/min.

With a similar approach, Prins et al. [11] modelled the mass loss of willow as a two step kinetic model under torrefaction conditions. As with Branca and di Blasi [10], all reactions were first order and followed the Arrhenius law. The kinetic parameters were identified under several isothermal tests at different temperatures, ranging from 230 to 300 °C with heat-up from 200 °C at 10–100 K/min and observation times of 3 h. The two step mechanism was shown to provide good results above 270 °C but no comparisons were shown for lower temperatures.

1.2. Models proposed for cellulose

The first kinetic model for cellulose was developed by Broido and Weinstein [12] for temperatures higher than 400 °C (Fig. 1). In the first step of this model, the cellulose generates some tar and anhydrocellulose, and in the second step the anhydrocellulose generates a solid and a gas phase. Later, Shafizadeh and Bradbury [13] modified this kinetic model with the hypothesis that the cellulose is first depolymerised or transformed into a more reactive phase (active cellulose) which is then transformed into three components: gas, tar and a solid residue. Currently, the most widely used model is the one proposed by Varhegyi et al. [14] (Table 2, scheme A) in which cellulose decomposes directly into gas and solid phases through two parallel reactions. Compared to the single first order reaction mentioned above (Eq. (1)) this kinetic representation allows the variations of product yields with temperature to be taken into account.

1.3. Models proposed for hemicelluloses

Hardwood hemicelluloses are mainly composed of xylan (~80%) whereas softwood hemicelluloses are mainly made of glucomannan (~60%) [4]. The latter is not as readily available commercially as the former, therefore studies on the thermal treatment of glucomannan are scare, and the literature mostly offers kinetic models for xylan. Just recently, Branca et al. [15] used a one and a two stage mechanism to describe the pyrolysis kinetics of commercial glucomannan.

It has long been considered that xylan thermal treatment follows an irreversible single-step first order reaction [16]. However, as shown above for wood, such kinetic schemes lead to rate coefficients that are temperature and heating rate dependent. Multi-step series kinetic models are therefore more adapted for xylan weight loss prediction. Several two or three step kinetic mechanisms have been proposed [17–21] which provide more accurate predictions of hemicelluloses mass loss during pyrolysis.

1.4. Models proposed for lignin

To our knowledge, the only kinetic model existing for lignin torrefaction is an irreversible single-step first order reaction. Several authors have identified kinetic parameters that vary according to the experimental conditions and the nature of lignin [17,22–25].

1.5. Summary

In light of the above review, the various kinetic models proposed for predicting the mass loss of lignocellulosic biomass, xylan,

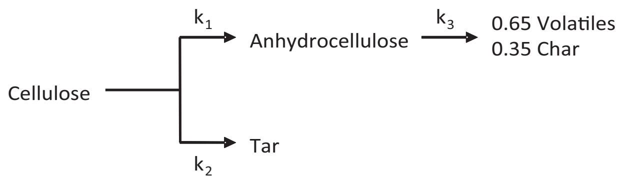

Fig. 1. Kinetic model of cellulose thermal treatment proposed by Broido and Weinstein [12].

Table 2
Summary of the main kinetic model existing on literature.

Kinetic model	Authors original scheme	Scheme
A	Varhegyi et al. [14] Koufopanos et al. [17] Tang et al. [22] William et al. [23] Gronli et al. [24] Orfao et al. [25]	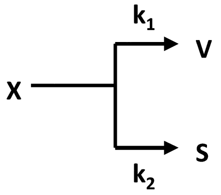
B	Prins et al. [11] Broido and Weinstein [12] Shafizadeh et al. [13] Varhegyi et al. [19] Lanzetta et al. [20] Fisher et al. [21]	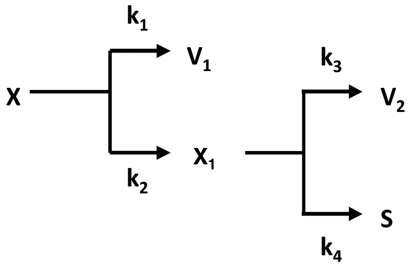
C	Branca et al. [10] Ward et al. [18]	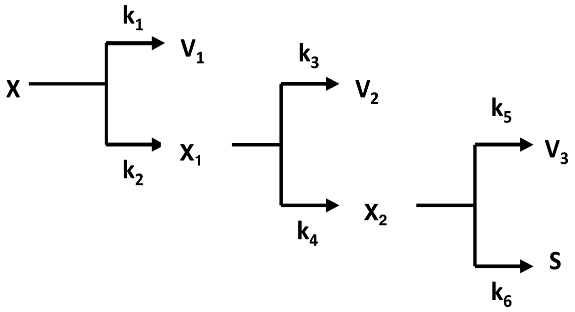 k1 V1 k3 X V2 k5 V3 X1 k2 X2 k4 S k6

cellulose and lignin during thermal treatment, can be categorized into three types, A, B or C respectively for single, two or 3-step reactions as listed in Table 2. For example, the model proposed by Ward et al. [18] (Fig. 2) for the thermal treatment of xylan is considered to be one of type C. This model gives the proportion of volatiles for each irreversible first order reaction, with $k_{v1}/(k_{v1}+k_{s1}) = 0.16$, $k_{v2}/(k_{v2}+k_{s2}) = 0.47$ and $k_{v3}/(k_{v3}+k_{s3}) = 0.36$.

The kinetic parameters determined from these models have mostly been identified under dynamic tests with final temperatures above 400 °C exceeding typical torrefaction conditions. Thus it is not readily clear which type of model and complexity is required for adequately reproducing the rate of mass loss under moderate thermal treatment. Targeting conditions more representative of torrefaction conditions, new weight loss measurements are presented here in the temperature range of 210–300 °C for various biomass and biomass component samples. The data are used to evaluate the different types of mechanistic schemes proposed in the literature by using an inverse method to evaluate optimized kinetic parameters for each scheme and for each sample, valid for the whole range of temperatures studied. The most adequate mechanistic schemes are thus identified for each sample.

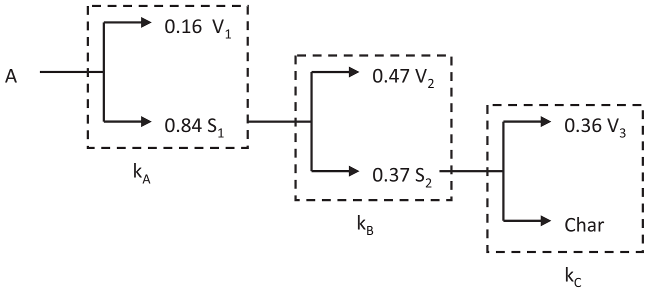

Fig. 2. Kinetic model for xylan thermal degradation developed by Ward et al. [18].

2. Materials and methods

2.1. Experiments

Mass loss during torrefaction was measured by TGA under a nitrogen flow of 15 mL/min in a Setaram thermo-balance (Sensys-evo-3D) with less than 1% error. The accuracy of the measurements was estimated from several blank tests to correct the effects of buoyancy forces which depend on the gas flow rate and the temperature level. Each sample is first dried at 100 °C for two hours then heated at 20 K/min up to a final temperature of 210 °C, 250 °C or 290 °C which is maintained for a period of ten hours. This protocol was designed to assess the kinetic rates under essentially isothermal conditions.

Three species of wood have been studied: locust, a temperate hardwood, spruce, a softwood, and eucalyptus, a tropical hardwood. They have been selected on the basis of their different structural properties which lead to different thermal resilience and thus possibly to different appropriate kinetic models. The weight loss of the main components of lignocellulosic biomass was also measured for cellulose (Sigma–Aldrich), xylan (Sigma–Aldrich), lignin (Green Value) and glucomannan (Kalys). The later is an important contribution of the present work as the literature is very poor in data regarding this important component of softwood. The polymers were supplied as powders, whereas the woody biomass

Table 3
Fraction of mass loss that occurs during the heating phase.

Temperature (°C)	Fraction of mass loss at the end of the heating period (%) (AWL(t = 10 h) (%))						
	Xylan	Glucomannan	Cellulose	Lignin	Spruce	Locust	Eucalyptus
210 °C	5.4 (26.1)[a]	0.8 (11.2)	≈0 (≈0)	4 (10.5)	1 (8)	0.8 (13.9)	1 (9.3)
250 °C	11.6 (51)	1 (51)	2.5 (15.5)	11.8 (17.2)	2.7 (33)	2.7 (33.3)	3.3 (33.8)
290 °C	34.7 (58.5)	3.6 (66.2)	0.7 (71.7)	13.6 (24.8)	3.9 (67.5)	6.1 (60.8)	6.5 (58.9)

[a] The first number is $\frac{AWL_{end\_heating}}{AWL_{10\,h}} \cdot 100$, the number in parentheses is $AWL_{10\,h}$ (%).

samples were ground to obtain particle sizes under 0.1 mm. Working with powders allowed heat transfer limitations to be neglected. The sample initial weight varied from 15 to 18 mg for polymers and from 6 to 9 mg for woody biomass.

2.2. Solution of the kinetics formulation

For accuracy purposes, all kinetic models were solved numerically in this work. This allows any time-temperature pathway to be solved with the actual conditions undergone by the sample. The method principle will be detailed for model C. The strategy is similar, and simpler, for models A and B (four differential equations for model B and only two for model A).

In the case of model C described in Table 2, the set of differential equations describing the evolution of the system are written as follows:

$$\frac{d[X]}{dt} = -(k_1 + k_2)[X] \quad (7)$$

$$\frac{d[V_1]}{dt} = k_1[X] \quad (8)$$

$$\frac{d[X_1]}{dt} = k_2[X] - (k_3 + k_4)[X_1] \quad (9)$$

$$\frac{d[V_2]}{dt} = k_3[X_1] \quad (10)$$

$$\frac{d[X_2]}{dt} = k_4[X_1] - (k_5 + k_6)[X_2] \quad (11)$$

$$\frac{d[V_3]}{dt} = k_5[X_2] \quad (12)$$

$$\frac{d[S]}{dt} = k_6[X_2] \quad (13)$$

$$m = [X] + [X_1] + [X_2] + [S] \quad (14)$$

where $[X]$ is the mass of the raw material, $[V_1]$, $[V_2]$ and $[V_3]$ are the mass of volatiles, $[S]$ is the mass of torrefied material, and $[X_1]$ and $[X_2]$ are the mass of intermediary components. All reactions are first order and kinetic rates k_1, k_2, k_3 and k_4 follow the Arrhenius law (Eq. (2)).

If fully isothermal reaction conditions were reached the analytical resolution of equations Eqs. (7)–(14) would have been possible. However, it is important to point out that the mass loss during the short heat-up phase is not systematically negligible. The ratio of this early mass loss relative to the total one observed after 10 h is specified in Table 3 for the various samples. The values are highest for xylan and lignin, exceeding 10% at temperatures above 250 °C.

Due to this early mass release, the kinetic parameters need to use the actual sample temperature. Therefore, the set of Eqs. (7)–(14) was solved numerically, using a Crank–Nicholson scheme, a second order finite difference method in time, as described hereafter:

$$\frac{d[X]}{dt} \approx \frac{[X]^{n+1} - [X]^n}{dt} \approx -0.5(k_1^{n+1} + k_2^{n+1})[X]^{n+1} - 0.5(k_1^n + k_2^n)[X]^n \quad (15)$$

$$\frac{d[V_1]}{dt} \approx \frac{[V_1]^{n+1} - [V_1]^n}{dt} \approx 0.5k_1^{n+1}[X]^{n+1} + 0.5k_1^n[X]^n \quad (16)$$

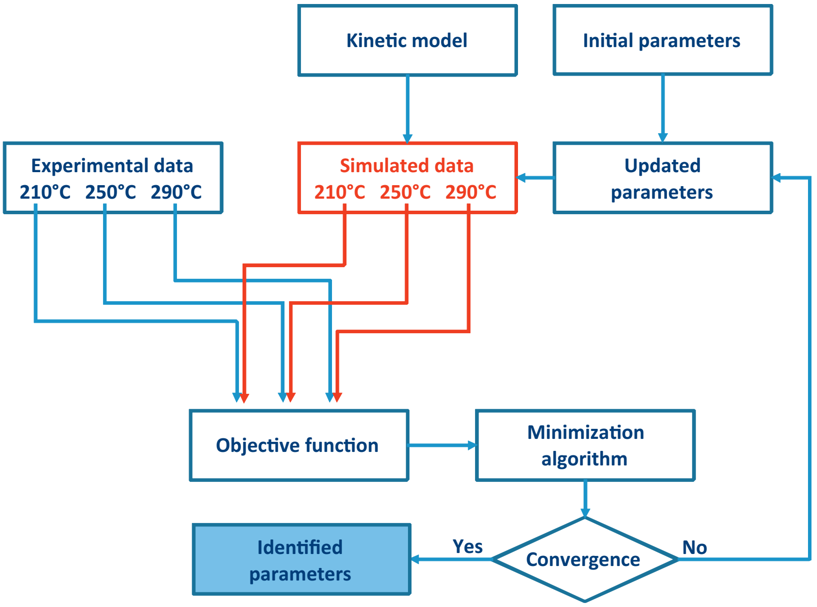

Fig. 3. Inverse method principle.

$$\frac{d[X_1]}{dt} \approx \frac{[X_1]^{n+1}-[X_1]^{n}}{dt} \approx 0.5(k_2^{n+1}[X]^{n+1} - (k_3^{n+1}+k_4^{n+1})[X_1]^{n+1}) + 0.5(k_2^{n}[X]^{n} - (k_3^{n}+k_4^{n})[X_1]^{n}) \tag{17}$$

$$\frac{d[V_2]}{dt} \approx \frac{[V_2]^{n+1}-[V_2]^{n}}{dt} \approx 0.5(k_3^{n+1}[X_1]^{n+1}) + 0.5(k_3^{n}[X_1]^{n}) \tag{18}$$

$$\frac{d[X_2]}{dt} \approx \frac{[X_2]^{n+1}-[X_2]^{n}}{dt} \approx 0.5(k_4^{n+1}[X_1]^{n+1} - (k_5^{n+1}+k_6^{n+1})[X_2]^{n+1}) + 0.5(k_4^{n}[X_1]^{n} - (k_5^{n}+k_6^{n})[X_2]^{n}) \tag{19}$$

$$\frac{d[V_3]}{dt} \approx \frac{[V_3]^{n+1}-[V_3]^{n}}{dt} \approx 0.5k_5^{n+1}[X_2]^{n+1} + 0.5k_5^{n}[X_2]^{n} \tag{20}$$

$$\frac{d[S]}{dt} \approx \frac{[S]^{n+1}-[S]^{n}}{dt} \approx 0.5k_6^{n+1}[X_2]^{n+1} + 0.5k_6^{n}[X_2]^{n} \tag{21}$$

In Eqs. (15)–(21), subscript n stands for time t and subscripts $n+1$ stands for tine $t+dt$. All kinetic parameters k_i are computed using the actual sample temperature (either time t or time $t+dt$), as obtained during the thermobalance tests.

2.3. Parameter evaluation by inverse method

Kinetic parameters were identified using an inverse method, the principles of which are summarized in Fig. 3. The originality of our approach is to fit a single set of parameter values using the three temperature levels simultaneously. A first set rate parameters with representative values are estimated and used to compute mass loss solutions for a given sample at the three temperatures. This computation uses the experimental temperature histories as input data. An objective function is defined as the error between experiments and data over the full experimental times at all temperatures and the optimization algorithm varies the parameter values to minimize this objective function. The objective function F used in the present work is defined as follows.

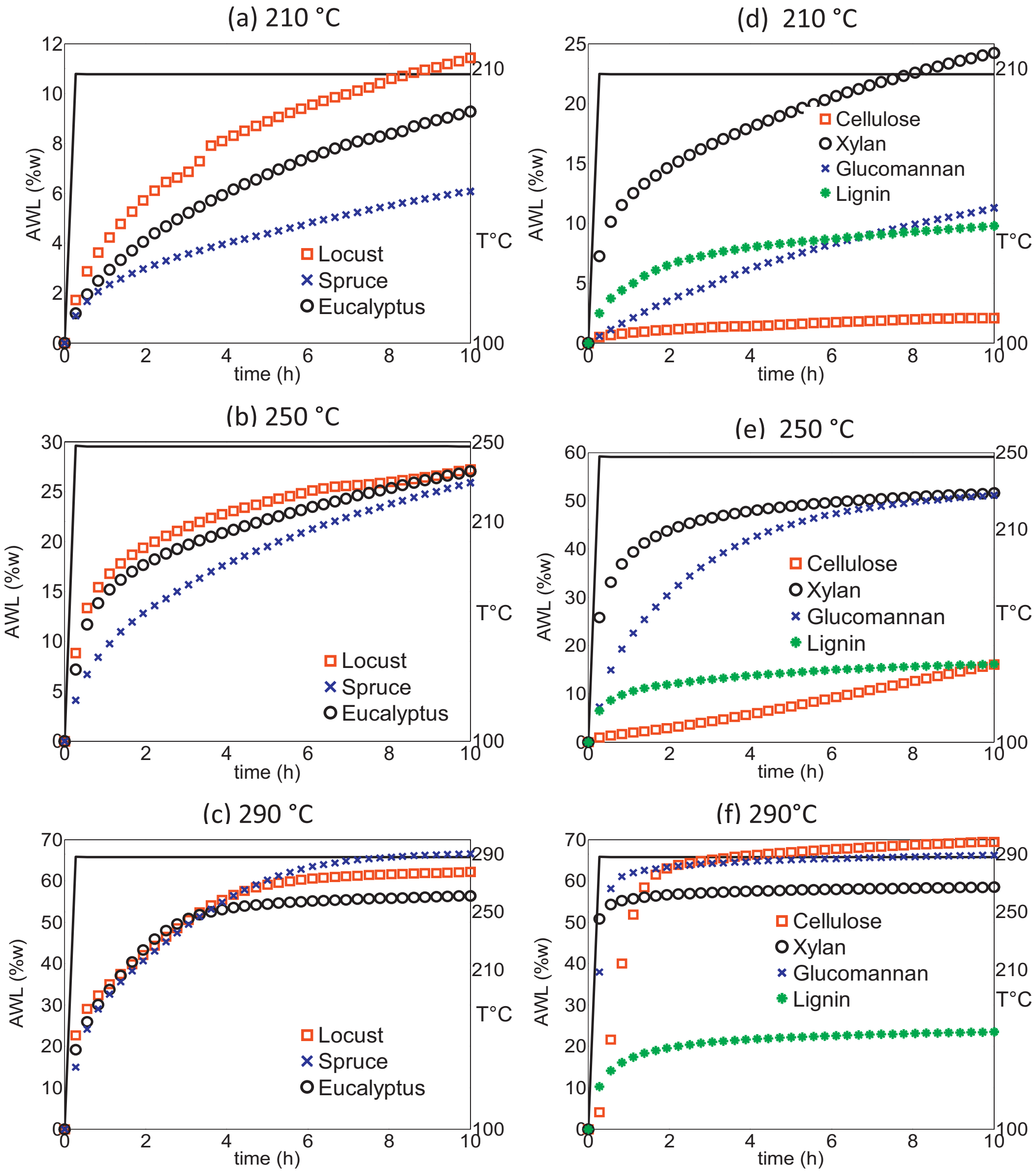

Fig. 4. Measured anhydrous weight loss (symbols) of: (a–c) wood samples (spruce, locust and eucalyptus) and (d–f) wood constituents (cellulose, xylan, glucomannan and lignin) for different temperatures (black lines).

$$F = \alpha_{210}F_{210} + \alpha_{250}F_{250} + \alpha_{290}F_{290} \tag{5}$$

where

$$F_T = 100\sqrt{\frac{\sum_{i=1}^{N^T}\left(m_{i,\text{observed}}^T - m_{i,\text{calculated}}^T\right)^2}{N^T\left(m_0^T\right)^2}} \tag{6}$$

and the α_T are weighting coefficients for the different temperature levels ($\sum \alpha_T = 1$). N^T is the size of the data vector at temperature T, m_0^T is the initial mass, $m_{i,\text{observed}}^T$ is the measured mass loss and $m_{i,\text{calculated}}^T$ is the corresponding calculated mass loss. As the total mass loss depends strongly on the temperature level (Fig. 4), the weighting coefficients α_T have to depend on the temperature level to minimize simultaneously the global error and the particular errors. The choice of these weighting coefficients was made to reduce the error at 210 °C while maintaining a good fit at the higher temperatures. A detailed description of the method derived to optimize the choice of the weighting coefficients is proposed in Section 3.2.

3. Results and discussion

3.1. Weight loss experiments

The anhydrous weight loss (AWL, defined as the ratio of the instantaneous mass loss as a function of time and the initial mass after drying) of spruce, locust and eucalyptus are compared at three different isothermal temperatures of 210 °C, 250 °C and 290 °C in Fig. 4a–c respectively. Similar results for the lignocellulosic biomass constituents, cellulose, xylan, glucomannan and lignin are shown in Fig. 4d–f.

The results display interesting relative behaviours between spruce, locust, xylan and glucomannan. At 210 °C locust shows a higher AWL than spruce in agreement with the observations of others [11,25]. This behaviour is explained by the different nature of hemicellulose in these samples. Locust hemicellulose is mainly composed of xylan, whereas spruce hemicellulose is mainly composed of glucomannan. As shown in Fig. 4a, at 210 °C, spruce is more thermally stable than locust. However, for long residence times, reaching 10 h, and with increasing temperatures, the AWL of spruce close to that of locust at 250 °C (Fig. 4b) eventually supersedes it at 290 °C (Fig. 4c). These relative characteristics are also observed for xylan and glucomannan which confirms the strong link between the reactivity of the wood and its composition in hemicelluloses. It should also be noted that softwood species, such as spruce or pine, are generally considered to exhibit lower weight losses than deciduous trees. However, few studies extend to residence times of 10 h and our results show that at temperatures above 250 °C this trend eventually reverses.

Finally, we note that lignin is the constituent that shows the least AWL variation with temperature and does not exhibit more than 20% AWL even at the highest temperature. In contrast, cellulose exhibits the strongest AWL loss with temperature (up to 70%). As expected from the literature [4] cellulose exhibits very low mass losses at moderate temperature levels (below 250 °C), but presents the highest mass loss value at 290 °C after 10 h of heat treatment. Nevertheless, the time constant for cellulose decomposition remains the largest one.

3.2. Choice of the weighting coefficients

The choice of the weighting coefficients α_T is discussed hereafter. Optimized kinetic parameters are found by minimizing the residue F. In principle we could have allowed free variation of the weight coefficients. However, this leads to poor results either for the higher or for the lower temperatures. Indeed, it was observed that kinetic parameters identified using only the test at 210 °C, fits correctly the anhydrous weight loss measured at 210 °C (low F_{210}), but underestimates the anhydrous weight loss at higher temperatures (high F_{250} and F_{290}). On the contrary, kinetic parameters identified at high temperature (250 or 290 °C) fit correctly the anhydrous weight loss at high temperatures (low F_{250} and F_{290}) but overestimate the weight loss at low temperature (high F_{210}). A constraint needs to be imposed to get a reasonable F_T for each temperature (lower than 5%) while still having a low F value. A new dimensionless number is then introduced as described in Eq. (22) where Z is the ratio between the weighting factor at low temperature (210 °C), α_{low}, and the weighting factor at high temperatures (250 and 290 °C), α_{high}.

$$Z = \frac{\alpha_{\text{Low}}}{\alpha_{\text{High}}} \tag{22}$$

Fig. 5a and b depicts the variation of the overall residue value (F) and of the residue values for each temperature level (F_T) as a function of Z for xylan (a) and locust (b) in the case of B-type scheme. It is observed that the lowest value of F is obtained for $Z = 0$, which is normal, because in this case the identification by inverse method does not take into account measurements at 210 °C ($\alpha_{210} = 0$), which allows the identification to focus on levels 250 °C and 290 °C. Consistently, the error found for level 210 °C is huge (more than 16% for the two examples depicted here). On the contrary, for large values of Z, the overall criterion is rather good, the residue for 210 °C excellent, but those for 250 °C and 290 °C unacceptable.

It is also observed that from $Z = 6$ for xylan and $Z = 6.5$ for locust, values of F_{210}, F_{250} and F_{290} become constant, while the overall residue value F is still decreasing. This is explained by the fact that for high Z values, the minimization algorithm practically does not take into account anymore the high temperature measurements. Indeed, as Z increases F decreases to a limit value which corresponds to F_{210} value when $F_{250} = F_{290} = 0$ (or $Z \to \infty$).

By observing the curves obtained for either locust or xylan, an optimum appears clearly in the region of $Z = 2$, for which both the global error and the individual errors remain below 5%. Therefore, the kinetic parameters presented hereafter have been evaluated with $\alpha_{210} = 0.5$ and $\alpha_{250} = \alpha_{290} = 0.25$.

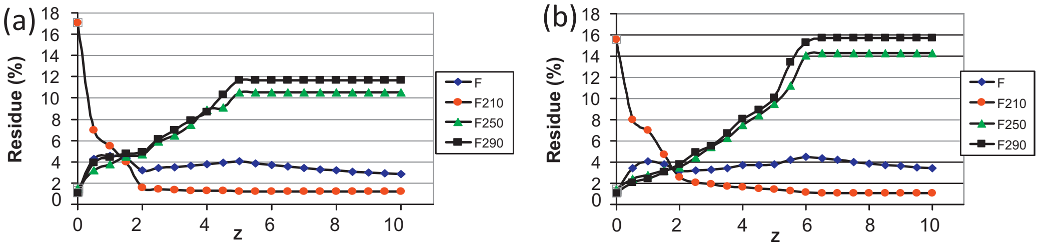

Fig. 5. Evolution of overall residue value, at 210 °C, 250 °C and 290 °C as a function of Z for xylan (a) and locust (b) with a type B kinetic model.

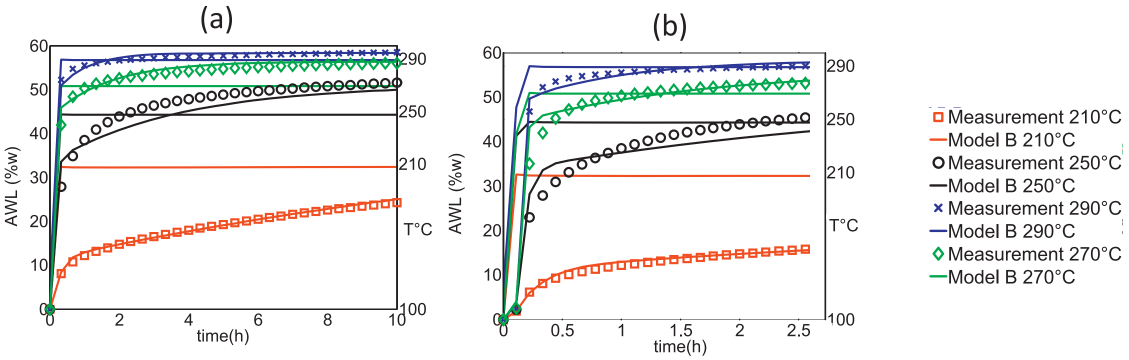

Fig. 6. Comparison between measured (symbols) and calculated (dashed lines) mass losses over long (a) and short (b) time scales for xylan using model type B at different temperatures (solid lines).

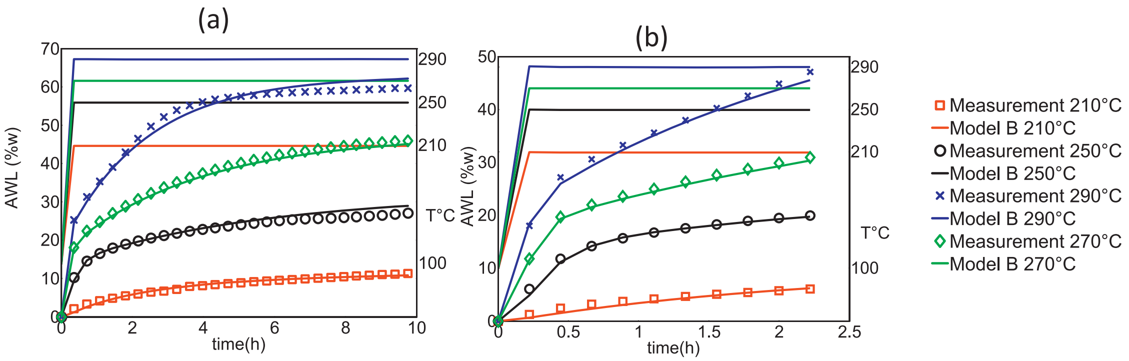

Fig. 7. Comparison between measured and calculated mass losses over long (a) and short (b) time scales for locust using model type B at different temperatures (solid lines).

3.3. *Assessment of the identified kinetic parameters*

Typical results for xylan and locust are presented in Figs. 6 and 7 in which the measured and predicted mass losses with a type-B model are compared. These figures prove that the identified kinetics are able to predict with good accuracy the measured mass loss of the samples throughout the entire experimental time, particularly for locust during the first hour, which includes the non isothermal heating phase (Fig. 7b), as well as up to ten hours (Fig. 7a).

In order to validate the model with data, the kinetic models were tested on experimental data not used in the identification process. Results for the anhydrous weight loss of xylan and locust at 270 °C has also been measured in order to verify the model with a set of data that was not used in the kinetic parameters identification, the heating rate between 100 °C and 270 °C being also 20 K/min. The computed mass loss using the experimental temperature history, according to kinetic parameters values identified with measurements at 210, 250 and 290 °C, is found to agree well with this data at 270 °C.

Finally, as further test of the quality of the proposed kinetics model, Fig. 8a and b represents the comparison between the measured and predicted mass loss rate ($d(\mathrm{AWL})/dt$) for locust and xylan, respectively, as a function of time with the type-B model. First, it is observed that a double peak of mass loss rate appears for xylan during thermal treatment at 290 °C, while no visible double peak exists during thermal treatment of locust. However, model B is able to predict with an acceptable accuracy the mass loss rate even in the case of two maximal values of mass loss rate.

The identified value of kinetic parameters for all samples are presented in Tables 4–6 for types A, B and C models respectively. For the wood samples, in the case of type B and C models, the first reaction step is fast and is not rate limiting. This result is in agreement with the findings of Lanzetta et al. [20] and Prins et al. [11], and is coherent with the fact that the first step should represent hemicelluloses decomposition whereas the last one accounts for cellulose decomposition.

The overall residue values obtained with models A, B and C are presented in Fig. 9 for all samples. It can be seen that models B and

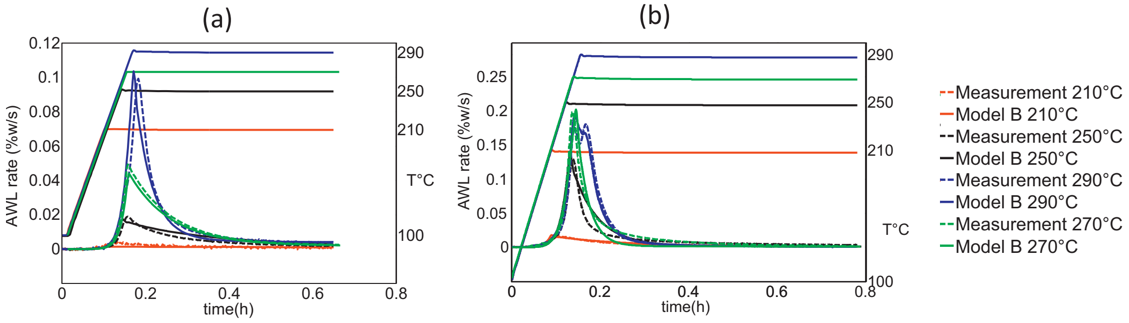

Fig. 8. Anhydrous weight loss rate (wt%/s) as a function of time for locust (a) and xylan (b) for all level of temperatures.

Table 4
Torrefaction kinetic parameters evaluated with a type-A model.

	Xylan	Cellulose	Glucomannan	Lignin	Locust	Eucalyptus	Spruce
A1 (s^{-1})	2.9×10^{9}	6.3×10^{17}	3.9×10^{10}	2.4×10^{7}	4.3×10^{5}	2.8×10^{5}	4.4×10^{8}
E1 (kJ/mol)	129.9	230.1	147.8	114.8	102.2	100.6	136.9
A2 (s^{-1})	2.9×10^{5}	4.2×10^{11}	4.1×10^{7}	3.1×10^{5}	0.15	3.5	1.78×10^{8}
E2 (kJ/mol)	89.2	168.1	118.5	88.7	34.9	48.9	135.9

Table 5
Torrefaction kinetic parameters evaluated with a type-B model.

	Xylan	Cellulose	Glucomannan	Lignin	Locust	Eucalyptus	Spruce
A1 (s^{-1})	2.2×10^{9}	1.2×10^{8}	1.7×10^{11}	3.45×10^{6}	4.1×10^{9}	9.3×10^{7}	1.4×10^{7}
E1 (kJ/mol)	121.7	233.8	153.4	102.9	133.9	119.2	113.2
A2 (s^{-1})	2.7×10^{2}	6.5×10^{9}	3×10^{7}	1.8×10^{5}	1.35×10^{7}	2.4×10^{3}	1.5×10^{3}
E2 (kJ/mol)	50.6	157.3	114.9	81.4	101.7	64.9	62.9
A3 (s^{-1})	91.7	28.3	2.7×10^{3}	1.24×10^{4}	9.9×10^{5}	4.3×10^{5}	1.6×10^{6}
E3 (kJ/mol)	66.6	61.3	87	96.9	110	106.4	112.6
A4 (s^{-1})	4.1×10^{4}	3.9×10^{3}	1.9×10^{5}	9.81×10^{3}	5.3×10^{-3}	5.2	7.7×10^{-3}
E4 (kJ/mol)	89.5	80.3	99	85.9	21.3	52.3	35.5

Table 6
Torrefaction kinetic parameters evaluated with a type-C model.

	Xylan	Cellulose	Glucomannan	Lignin	Locust	Eucalyptus	Spruce
A1 (s^{-1})	2.06×10^{9}	1.29×10^{19}	3.58×10^{12}	2.6×10^{7}	3.9×10^{9}	1.7×10^{7}	1.2×10^{7}
E1 (kJ/mol)	120.4	244.4	166.3	108.9	131.9	112	111.4
A2 (s^{-1})	53	6.93×10^{9}	1.19×10^{7}	2.2×10^{4}	1.2×10^{7}	628.2	1.6×10^{3}
E2 (kJ/mol)	43	145.1	108.5	76.3	100.2	58.7	62.5
A3 (s^{-1})	2.36×10^{2}	34.02	488.34	1.3×10^{4}	9.7×10^{5}	1.1×10^{6}	1.5×10^{6}
E3 (kJ/mol)	70.3	75.8	74	86.2	108	110.1	113.1
A4 (s^{-1})	4.09×10^{4}	8.44×10^{3}	2.95×10^{5}	1.2×10^{4}	6.3×10^{-3}	15.9	7.8×10^{-3}
E4 (kJ/mol)	88.3	78.7	97.9	75.1	20.3	56.4	37.9
A5 (s^{-1})	1.42×10^{4}	7.9×10^{4}	1.75×10^{4}	9.6×10^{3}	1.3×10^{4}	1×10^{5}	5.1×10^{5}
E5 (kJ/mol)	269.9	93.7	198.1	97.7	101	106.6	100
A6 (s^{-1})	7.28×10^{2}	5.79×10^{5}	2.07×10^{4}	$4.9\ 10^{3}$	1.5×10^{4}	4.2×10^{4}	6.3×10^{4}
E6 (kJ/mol)	48.4	101.2	205.3	84.5	90.1	513.4	78

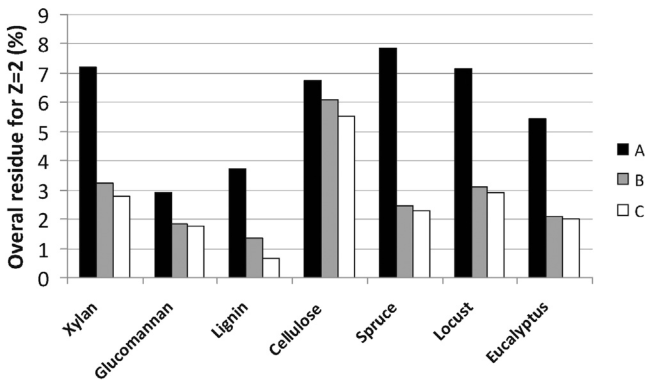

Fig. 9. *F* values for kinetic model A, B and C for all samples with $Z = 2$.

C always give a lower residue than model A which means that models B and C allow a better prediction of the mass loss than model A. In addition, model C does not significantly decrease the residue compared to model B, except for lignin. Therefore model B is recommended for xylan, glucomannan, cellulose, spruce, locust and eucalyptus and model C for lignin.

In the case of cellulose, one can see that the residue with model types B and C remain high compared to those obtained for the others samples. The main difficulty is that these kinetic schemes do not allow a proper description of cellulose depolymerisation when the treatment temperature approaches 300 °C. Some form of parallel reaction step is possibly required, and more sophisticated mechanism should be developed to improve predictions.

4. Conclusion

The anhydrous weight loss (AWL) during isothermal treatment under inert atmosphere of three woody biomasses (locust, spruce and eucalyptus) and their main components (xylan, glucomannan, lignin and cellulose) have been measured using an accurate thermobalance (Sensys-evo 3D). We observed that the higher mass loss rate observed in locust compared to spruce can be partially explained by the higher reactivity of xylan (main component of locust hemicelluloses) relative to that of glucomannan (main component of spruce hemicelluloses) only for moderate treatment intensity. At high temperatures (290 °C) and long residence times (5 h) spruce decomposition is stronger due to both higher cellulose and glucomannan reactivities.

Based on this comprehensive set of experimental data, kinetic models suitable for implementation into a macroscopic computational model [26,27] have been evaluated. The kinetic parameters for multi-step series reaction mechanisms found in the literature (1, 2 and 3 step-models) have been evaluated by an inverse method. This method computes the solution of the multi-step formulation using the experimental temperature histories undergone by the samples as input data. In addition, the inverse procedure takes into account simultaneously the three temperature levels for all samples, resulting in a prediction model valid in the whole studied temperature range.

The results show that the accuracy of a 2-step series reaction model is generally satisfactory for representing the mass loss of lignocellulosic biomass and their components. The gains from a more complex 3-step model are not sufficient to warrant the added complexities. It therefore appears that further improvements in thermal decomposition models in this temperature range would require other kind of kinetic schemes.

Further work is currently undertaken to test the potential of these formulations when implemented in our comprehensive heat and mass transfer computational model [28], both at the micro-particle scale at different temperatures as well as at the macroscopic scale of a fixed bed reactor.

Acknowledgement

The authors wish to thank the Fondation Tuck (ENERBIO program) which funded the salary of the PhD student involved in this work.

References

[1] T.G. Bridgeman, J.M. Jones, A. Williams, D.J. Waldron, An investigation of the grindability of two torrefied energy crops, Fuel 89 (2010) 3911–3918.

[2] C. Tapas., T.C. Acharjee, C.J. Coronella, V.R. Vasquez, Effect of thermal pretreatment on equilibrium moisture content of lignocellulosic biomass, Bioresource Technology 102 (2011) 4849–4854.

[3] G. Almeida, J.O. Brito, P. Perré, Changes in wood–water relationship due to heat treatment assessed on micro-samples of three *Eucalyptus* species, Holzforschung 63 (2009) 80–88.

[4] P.C.A. Bergman, A.R. Boersma, J.H.A. Kiel, M.J. Prins, K.J. Ptasinski, F.J.J.G. Janssen, Torrefaction for entrained-flow gasification of biomass, 2005, Technical ECN Report.

[5] G. Almeida, J.O. Brito, P. Perré, Alterations in energy properties of eucalyptus wood and bark subjected to torrefaction: the potential of mass loss as a synthetic indicator, Bioresource Technology 101 (2010) 9778–9784.

[6] W.M. Wendlandt, Thermal Analysis, 3rd ed., John Wiley & Sons, New York, 1986.

[7] D.K. Shen, S. GU, A.V. Bridgewater, Study on the pyrolytic behaviour of xylan-based hemicellulose using TG-FTIR and Py-GC-FTIR, Journal of Analytical and Applied Pyrolysis 87 (2010) 199–206.

[8] D.B. Anthony, J.B. Howard, H.C. Hottel, H.P. Meissner, Rapid devolatilization of pulverized coal, in: Fifteenth Symposium (International) on Combustion, 15, 1975, pp. 1303–1317.

[9] G. Varhegyi, B. Bobali, E. Jakab, H. Chen, Thermogravimetric study of biomass pyrolysis kinetics. A distributed activation energy model with prediction tests, Energy and Fuels 25 (2011) 24–32.

[10] C. Branca, C.D. di Blasi, Kinetics of the isothermal degradation of wood in the temperature range 528–708 K, Journal of Analytical and Applied Pyrolysis 67 (2003) 207–219.

[11] M.J. Prins, K.J. Ptasinski, F.J.J.G. Janssen, Torrefaction of wood. Part 1. Weight loss kinetics, Journal of Analytical and Applied Pyrolysis 77 (2006) 28–34.

[12] A. Broido, M. Weinstein, Low temperature isothermal pyrolysis of cellulose, Combustion Science and Technology 3 (1971) 285–296.

[13] F. Shafizadeh, A.G.W. Bradbury, Thermal degradation of cellulose in air and nitrogen at low temperature, Journal of Applied Polymer Science 23 (1979) 1431–1441.

[14] G. Varhegyi, E. Jakab, M.J. Antal, Is the Broido-Shafizadeh model for cellulose pyrolysis true? Energy and Fuels 8 (1994) 1335–1352.

[15] C. Branca, C. Di Blasi, C. Mango, I. Hrablay, Products and kinetics of glucomannan pyrolysis, Industrial and Engineering Chemistry Research 52 (2013) 5030–5039.

[16] P. Rousset, I. Turner, A. Donnot, P. Perré, Choix d'un modèle de pyrolyse ménagée du bois à l'échelle de la microparticule en vue de la modélisation macrocospique, Annals of Forest Science 63 (2006) 213–229.

[17] C.A. Koufopanos, G. Mashio, A. Lucchesi, Kinetic modeling of the pyrolysis of biomass and biomass component, Canadian Journal of Chemical Engineering 67 (1989) 75–94.

[18] S.M. Ward, J. Braslaw, Experimental weight loss kinetics of wood pyrolysis under vacuum, Combustion and Flame 61 (1986) 261–269.

[19] G. Varhegyi, M.J. Antal, E. Jakab, P. Szabo, Kinetic modeling of biomass pyrolysis, Journal of Analytical and Applied Pyrolysis 42 (1997) 73–87.

[20] M. Lanzetta, C.D. Di Blasi, Intrinsic kinetics of isothermal xylan degradation in inert atmosphere, Journal of Analytical and Applied Pyrolysis 40 (1997) 287–303.

[21] T. Fisher, Pyrolysis behavior and kinetics of biomass derived materials, Journal of Analytical and Applied Pyrolysis 62 (2002) 331–349.

[22] W.K. Tang, Effect of Inorganic Salts on Pyrolysis of Wood, Alpha Cellulose and Lignin, USDA Forest Product Laboratory, 1967, FPL Research Paper No. 71.

[23] P.T. Williams, S. Besler, Thermogravimetric analysis of the component of biomass, in: A.V. Bridgewater (Ed.), Advances in Thermochemical Biomass Conversion, Blackie Academic & Professional, London, 1994.

[24] M.G. Gronli, A theorical and experimental study of the thermal degradation of biomass pyrolysis, wood, tar, char, Trondheim University, 1996, pp. 342 (PhD thesis).

[25] J.J.M. Orfao, J.L. Figueiredo, A simplified method for determination of lignocellulosic materials pyrolysis kinetics from isothermal thermogravimetric experiments, Thermochimica Acta 380 (2001) 67–78.

[26] V. Repellin, A. Govin, M. Rolland, R. Guyonnet, Energy requirement of torrefied wood, Biomass and Energy 34 (2010) 923–930.

[27] I.W. Turner, P. Rousset, R. Rémond, P. Perré, An experimental and theoretical investigation of the thermal treatment of wood in the range 200–260 °C, International Journal of Heat and Mass Transfer 53 (2010) 715–725.

[28] P. Perré, R. Rémond, I.W. Turner, A comprehensive dual-scale wood torrefaction model: application to the analysis of thermal run-away in industrial heat treatment processes, International Journal of Heat and Mass Transfer 64 (2013) 838–849.